Journal of Anatomy

J. Anat. (2019) **235**, pp903–911 doi: 10.1111/joa.13062

Ontogenetic changes of geometrical and mechanical characteristics of the avian femur: a comparison between precocial and altricial birds

Xinsen Wei and Zihui Zhang

College of Life Sciences, Capital Normal University, Beijing, China

Abstract

The mechanical performance of limb bones is closely associated with an animal's locomotor capability and is thus important to our understanding of animal behaviour. This study combined a geometrical analysis and three-point bending tests to address the question of how the mechanical performance of the femurs of Japanese quail (*Coturnix coturnix japonica*) and pigeon (*Columba livia domestica*) respond to changing functional demands during ontogeny. Results showed that hatchling quails had stiff bone tissues, and the femoral ultimate loads scaled negatively with body mass, corresponding to high functional demands during early growth. The hatchling pigeon femora had weak material properties but they showed a dramatic increase in Young's modulus during growth. Consequently, although femoral cross-sectional geometry showed negative allometry, the ultimate loads scaled positively with body mass. Older pigeons had more circular bone cross-sections than younger pigeons, probably due to load stimulation changes occurred shortly after the onset of locomotion. Negative allometry and isometry of the cross-sectional geometry of hind limb bones were observed in flying birds and ground-dwelling birds, respectively. The correspondence between geometrical change and locomotor pattern suggests that ontogenetic changes in cross-sectional geometry may be an effective indicator of avian locomotor behaviour.

Key words: avian femur; cross-sectional geometry; mechanical test; ontogenetic scaling; Young's modulus.

Introduction

An animal faces different locomotor-related functional demands at different ontogenetic stages. As critical locomotor structures, limb bones must be sufficiently robust to meet locomotor demands (Biewener, 1982; Blob, 2000; Ruff et al. 2006). Therefore, understanding mechanical performance changes in limb bones during growth might shed light on ontogenetic patterns and changes of life history. Skeletal mechanical performance depends on material properties of bone tissue and bone structural properties simultaneously (Spatz et al. 1996; Currey, 2003). Material properties of a tissue are inherent properties that describe how the tissue behaves. Specific features (i.e. geometry) have no effect on material properties. During early ontogenetic stages, bone tissue typically has a low density due to the low mineral content of the bone (Currey, 2002). In addition, rapidly growing bones are mainly composed of woven bone tissue instead of lamellar bone tissue (Carrier & Leon, 1990; Currey, 2003). With growth, increases in bone mineralization and density change material properties (Currey, 2002).

Long bone structural properties mainly depend on bone length and diaphyseal cross-sectional geometry. The moment arm in bending and torsion is proportional to bone length (Selker & Carrier, 1989; Habib & Ruff, 2008). Diaphyseal cross-sectional geometry affects a bone's resistance to loads. Specifically, the cross-sectional area (CSA) and second moment of area (SMA) indicate resistance to axial and bending loads, respectively, and the polar moment of area (PMA) reflects the overall bending and torsional resistance (Selker & Carrier, 1989; Currey, 2002; Lieberman et al. 2004). Studies have suggested that bone length is likely genetically determined, whereas bone cross-sectional geometry is more sensitive to load stimulation, especially during growth (Lanyon, 1980; Selker & Carrier, 1989; Ruff, 2003; Habib & Ruff, 2008; Nadell, 2017).

Carrier (1983) observed strong negative allometry of the cross-sectional geometry of long-bones during ontogeny in hares. The author suggested that modifying limb bone geometry may compensate for weak, immature bone tissue

Correspondence
Zihui Zhang, College of Life Sciences, Capital Normal University, Beijing 100048, China. T: + 86 10 68901020; F: + 86 10 68980851; E: zihuizhang@cnu.edu.cn

Accepted for publication *21 June 2019*
Article published online *29 July 2019*

© 2019 Anatomical Society

to enhance bone mechanical performance in young hares. The relatively more robust limb bones help young hares meet the requirements of high locomotor performance in response to higher predation pressures. A similar situation has been observed in many mammalian species (Carrier, 1983; Heinrich et al. 1999; Lammers & German, 2002; Main & Biewener, 2004), so it is considered a common ontogenetic characteristic in most mammals (Carrier, 1996; Herrel & Gibb, 2006). In contrast, the hind limb long bones show different allometric patterns in birds. Studies have observed negative allometry of cross-sectional geometry in the hind limb bones of California gulls and black noddies (Carrier & Leon, 1990; Bennett, 2008), whereas emu and greater rhea exhibited isometric or slightly positive allometric scaling relationships (Main & Biewener, 2006, 2007; Picasso, 2011).

Birds are unique in terms of their specializations for flying and bipedal locomotion (Dumont, 2010; Abourachid & Höfling 2012). Whereas most mammals live on the ground throughout their lives, most birds develop from hind limb-dominated juveniles into forelimb-dominated adults, although a few species prefer terrestrial locomotion (Gatesy & Middleton, 1997; Jackson et al. 2009). The unique locomotor behaviours might contribute to the different ontogenetic patterns of avian bones. However, the geometrical and mechanical differences between precocial and altricial birds, and the kinds of morphological variation that occurs during postnatal growth, remains unclear. It is, therefore, necessary to study ontogeny across a broad range of avian species and to conduct interspecific comparisons to clarify bone ontogenetic patterns. In this study, we focused on two avian species, the Japanese quail (*Coturnix coturnix japonica*) and pigeons (*Columba livia domestica*), which are significantly different in hatching maturity and locomotor behaviour. We performed a geometric analysis and mechanical tests to quantify the femoral mechanical performance of the femora in the two species.

The Japanese quail is a typical ground-dwelling precocial bird. Hatchlings have well-developed hind limbs and can walk and run a few hours after hatching. Although adults are able to fly a short distance, they prefer to avoid danger by running rather than flying (Ricklefs, 1979). Pigeons, on the other hand, are altricial birds; that is, they depend on their parents for food and protection during early growth. They cannot fly until fully grown, at about 4 weeks old. Pigeons use their hind limbs to dig and forage, but their primary locomotor pattern is flying.

Materials and methods

Thirty pigeons were collected at the age of 4, 7, 14, 21, 28, 56, 112, 168, 252 and 336 days (n = 3 for each age) from a commercial farm located in Beijing, China. The pigeons were weighed (M_B) immediately after collection; their entire right femora were dissected, and the bone length (L) was measured using a digital calliper (± 0.01 mm). All the connective tissue was removed. The femora were wrapped in gauze soaked in saline solution and then frozen at −20 °C to keep them from degradation, which may alter the inherent mechanical properties of the specimen.

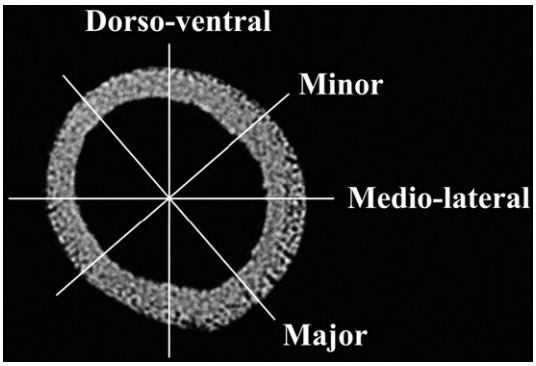

Fig. 1 Principal axes (major axis and minor axis) and anatomical axes (medio-lateral axis and dorso-ventral axis) of the femoral diaphysis. The major axis orients along the direction of maximum second moment of area of femoral cross-section. The minor axis is perpendicular to the major axis.

Entire right femora (dried specimens) of 51 quails were collected from the Laboratory of Ornithology, Capital Normal University, Beijing, China. The quails were 2, 4, 6, 8, 11, 14, 17, 20, 23, 27, 31, 35, 42, 49, 65, 97 and 134 days old (n = 3 for each age).

All femora were scanned using a Skyscan 1172 micro-computed tomography (μCT) scanner (Beijing Institute of Technology, Beijing, China) at a resolution of 15 μm pixel^{-1}. The femora were aligned with the scanner's vertical axis. Image data were reconstructed using NRecon v. 1.7 to acquire femoral cross-sectional images. Next, image stacks were imported into ImageJ 1.51, and the plug-in Bone J (Doube et al. 2010) was used to measure the CSA, periosteal diameter of diaphysis (D) and SMA (I) across all slices in each stack. Because of the irregular shape of the femoral cross-section (Fig. 1), the periosteal diameter of the diaphysis (D_{ml}, D_{dv}) and SMA (I_{max}, I_{min}, I_{ml}, I_{dv}) were measured along the principal axes (major axis, minor axis) and/or anatomical axes [mediolateral (ml) and dorsoventral (dv) axes], respectively. The PMA (J) was calculated as $I_{max} + I_{min}$ (Nadell, 2017). Finally, the average values of cross-sectional parameters of the entire diaphysis and midshaft were calculated. The middle segment with a length of 10% of the femur length was the midshaft (Fig. 2A).

Ontogenetic changes of bone circularity are thought to be closely associated with hind limb loads (Carlson & Judex, 2007; Nadell, 2017). The I_{max}/I_{min} and I_{ml}/I_{dv} ratios were calculated as the principal and anatomical circularity, respectively. Principal circularity was used as an indicator of bone cross-sectional shape, and anatomical circularity was used to estimate the dv/ml bending resistance ratio (Carlson & Judex, 2007; Nadell, 2017).

Bone structural strength indices

Bending and torsional loads, especially bending loads, are major components of hind limb loads in most birds and mammals (Biewener, 1982; Blob & Biewener, 1999; Main & Biewener, 2006). The bending moment and torsional moment are considered to be proportional to the product of body mass (M_B) and bone length (L; Currey, 2002; Habib & Ruff, 2008). Therefore, the stresses can be calculated as follows:

© 2019 Anatomical Society

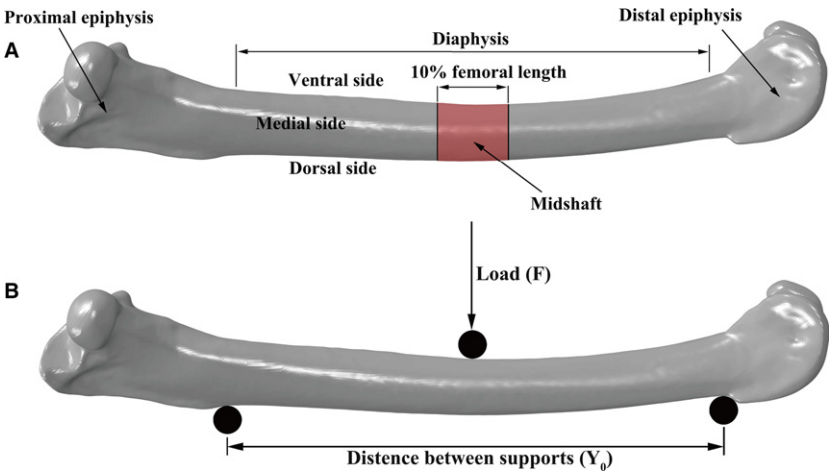

Fig. 2 Illustrations of femoral diaphysis and three-point bending test. (A) The diaphysis is defined as the shaft between obturator ridge end and proximal end of condyles; the middle segment of diaphysis with a length of 10% of the femur length is treated as the midshaft. (B) A schematic overview showing three-point bending test. The femora were loaded along the dv direction at the midshaft of the femur, and the supports were placed at the two ends of diaphysis.

$$\text{Bending stress} = M_B LD/2I = M_B/(2I/LD),$$

$$\text{Torsional stress} = M_B LD/2J = M_B/(2J/LD),$$

where I is the SMA, J is the PMA, and D is the diaphyseal diameter. For a given body mass, an individual with a high I/LD (J/LD) would undergo a low bending stress (torsional stress). I/LD and J/LD were, therefore, adopted as the bone structural strength index (BS) and polar bone structural strength index (PBS), respectively, to estimate bone structural properties (Currey, 2002; Habib & Ruff, 2008):

$$\text{BS} = I/LD,$$

$$\text{PBS} = J/LD.$$

PBS was an indicator of torsional resistance and overall bending resistance of femora, and BS_{ml} and BS_{dv} (BS along the anatomical axes. Fig. 1) are indicators of bending resistance in specific orientations.

Ultimate load and Young's modulus

Femoral ultimate load (F_u) and Young's modulus (E) were estimated by three-point bending tests. All femora were loaded to failure in an Instorn 5985 material-testing machine (Beijing Institute of Technology, Beijing, China). The femora were loaded along the dv direction (Fig. 2B) at the midpoint of the diaphysis, with the loading points displacing at a rate of 1.27 mm s^{-1} (Carrier, 1983; Jepsen et al. 2015). Femora of six quails aged 2 and 4 days were small and had weak bone tissue, so precise data were difficult to obtain, and these six femora were excluded from the three-point bending tests.

Young's modulus was calculated to estimate bone material properties (Spatz et al. 1996; Currey, 2002). For each femur, two points (1 and 2), located in the initial, straight part of the load-deformation curve, were selected, and the stress and strain of the two points were calculated by standard beam formulas:

$$\text{Stress} = F_u L_0 Y/(8I),$$

$$\text{Strain} = 6YH/L_0^2,$$

where F_u is the ultimate load, L_0 is the distance between supports, Y is the periosteal radius at midshaft, I is the SMA at midshaft, and H is bone deflection at the ultimate load point (Carrier & Leon, 1990; Spatz et al. 1996; Currey, 2002). The Young's modulus (E) was calculated by the stress difference/strain difference ratio of the two points:

$$E = (\text{Stress}_1 - \text{Stress}_2)/(\text{Strain}_1 - \text{Strain}_2).$$

Dehydration has a significant effect on bone material properties, where the Young's modulus of wet bone is about two-thirds that of dried bone (Silva et al. 2005). As we used dried quail femora in this study, we mainly focused on their ontogenetic changes instead of comparing the material properties between the two species.

Statistical analyses

Scaling relationships of measurements against body mass were calculated using SMATR 2.0. Allometric equations were calculated using the reduced major axis method. The data were $\log_{10}$-transformed, and linear regression was performed to define scaling relationships in the form of $\log y = b\log M_B + \log a$, where y refers to femoral measurements, a is the proportionality coefficient, b is the scaling exponent, and M_B is the body mass (Dytham, 2003). Significant differences in slope were based on 95% confidence intervals (CI), and $P < 0.05$ was considered statistically significant. Because the body mass grows rapidly before the young birds reach adult size, we included young birds (4–28 days old in pigeons and 2–35 days old in quails) in the juvenile group. The overall group contained both juveniles and adults. Scaling relationships in the juvenile group were calculated separately.

Differences in measurements were determined by analysis of variance, and the region, orientation and age group were considered

© 2019 Anatomical Society

the independent variables. The least significant difference and Student–Newman–Keuls *post hoc* tests were conducted to examine specific differences using SPSS Statistics V22.0 (IBM, Armonk, NY, USA). When the test of homogeneity of variances between groups was not satisfied, we used the nonparametric *post hoc* Mann–Whitney *U*-test (Dytham, 2003). $P < 0.05$ was considered statistically significant.

Results

The body mass and femoral length were ~ 4 and ~ 30% of the adult one, respectively, in 2-day-old quails, and 9 and 38% of adults', respectively, in 4-day-old quails. In contrast, the body mass and femoral length of 4-day-old pigeons were ~ 12 and ~ 48% of that in adults, respectively. Quails and pigeons grow rapidly during early ontogeny, and the growth stabilized after maturity. Femoral length exhibited positive allometry against body mass in both species (quails: $b = 0.392$ and $R^2 = 0.978$; pigeons: $b = 0.370$ and $R^2 = 0.972$; Table 1), especially in the juvenile group (quails: $b = 0.415$ and $R^2 = 0.978$; pigeons: $b = 0.381$ and $R^2 = 0.985$). We observed a gradual increase of femoral ultimate load in both quails and pigeons. The femoral ultimate load increased sevenfold during ontogeny in quails; however, the quails' body mass increased 24 times in the same period. In contrast, the femoral ultimate load increased by 15 times and the body mass by only seven times in pigeons. However, the allometric trends were different. In quails, the femoral ultimate load exhibited strong negative allometry against body mass (overall group: $b = 0.738$ and $R^2 = 0.873$; juvenile group: $b = 0.753$ and $R^2 = 0.825$; Table 1), whereas pigeons showed slightly positive allometry in the overall group ($b = 1.229$, $R^2 = 0.846$) but isometry in the juvenile group ($b = 0.932$, $R^2 = 0.928$).

Ontogenetic changes in structural properties

In quails, the dv periosteal diameter exhibited positive allometry against body mass, whereas the CSA, SMA and PMA scaled isometrically against body mass (Table 1). The juvenile group had the same allometric patterns as the overall group in all cross-sectional parameters but with a higher scaling slope, reflecting the high growth rate in the immature stage. Among the three bone structural strength indices, BS_{dv} scaled with slightly negative allometry against body mass, whereas BS_{ml} and PBS scaled isometrically against body mass (Table 1). In the juvenile group, PBS, BS_{ml} and BS_{dv} all scaled isometrically against body mass but with a larger slope when compared with the overall group.

In pigeons, all cross-sectional parameters (periosteal diameter, CSA, SMA and PMA) exhibited strong negative allometry against body mass (Table 1). The juvenile group showed a similar allometric pattern as the overall group, and the scaling slope was similar in both groups as well. BS_{ml}, BS_{dv} and PBS showed strong negative allometry against body mass in both groups.

Ontogenetic changes in cross-sectional circularity

In quails, femoral principal circularity (1.43 ± 0.10) showed no obvious change with age. Higher values (1.45 ± 0.11) were observed in 2- to 20-day-old quails, whereas the average value of the remaining quails was 1.41 ± 0.09, but there was no significant difference between them ($P = 0.119$). Femoral anatomical circularity (1.07 ± 0.11) was approximately constant during growth. I_{ml} was larger than I_{dv}, indicating a higher bending resistance in the dv direction. Although I_{max} was significantly higher than I_{min} ($P = 0.023$), no significant difference was found between I_{ml} and I_{dv} ($P = 0.606$).

Pigeons had a smaller principal circularity (1.41 ± 0.14) compared with quails, but the difference was not statistically significant ($P = 0.200$). The femoral principal circularity of pigeons ≤ 2 weeks old (1.58 ± 0.13) was significantly larger than older pigeons (1.34 ± 0.06; $P < 0.001$), suggesting that the femoral diaphysis was more elliptical in the younger pigeons. The anatomical circularity (0.82 ± 0.08) was < 1, indicating a larger resistance in ml orientation than in dv direction. The anatomical circularity in pigeons less than 2 weeks old (0.73 ± 0.07) was significantly smaller than in older pigeons (0.86 ± 0.05; $P = 0.002$), reflecting an increase in dorso-ventral bending resistance relative to medio-lateral bending resistance.

Ontogenetic changes in Young's modulus

The Young's modulus in quails increased by ~ 1.4 times from 6-day-olds to adults (from 7.7 ± 0.4 to 18.6 ± 2.4 GPa) and almost reached the adult level at day 35 after hatching (17.5 ± 0.8 GPa).

Pigeons had a dramatic increase in Young's modulus during growth. The Young's modulus of 4-day-old pigeons (95.2 ± 8.8 MPa) was only ~ 0.7% compared with adults (13.4 ± 3.0 GPa) but increased by ~ 18 times (1.8 ± 0.5 GPa) in the first 2 weeks and then by ~ 6 times from 2 weeks to maturity. Thus, Young's modulus in pigeons increased by ~ 140 times during ontogeny.

Discussion

Ontogenetic changes in femoral mechanical performance

In quails, the negative allometry of femoral ultimate load (Table 1) suggests that juvenile quail femora are more robust than those of adults. As ground-dwelling precocial birds, Japanese quails can walk within a few hours after hatching (Ricklefs, 1979) and they have to live independently. For most vertebrates, juveniles undergo high levels of predation due to their lower

© 2019 Anatomical Society

Table 1 Ontogenetic scaling of measurements vs. body mass in quails and pigeons.

Parameters	*n*	R^2	*P*-value	*b*	LowCI	UppCI	Interc
Quail							
L	51	0.978	0.000	**0.392+**	0.375	0.409	0.750
D_{ml}	51	0.968	0.000	0.331	0.315	0.348	−0.264
D_{dv}	51	0.968	0.000	**0.351+**	0.333	0.369	−0.287
CSA	51	0.873	0.000	0.598	0.540	0.662	−0.808
I_{max}	51	0.944	0.000	1.279	1.195	1.368	−2.314
I_{min}	51	0.952	0.000	1.289	1.211	1.373	−2.487
I_{ml}	51	0.94	0.000	1.297	1.209	1.391	−2.403
I_{dv}	51	0.953	0.000	1.269	1.193	1.351	−2.382
J	51	0.948	0.000	1.282	1.201	1.369	−2.089
BS_{ml}	51	0.852	0.000	0.599	0.537	0.669	−2.677
BS_{dv}	51	0.889	0.000	**0.591−**	0.538	0.651	−2.683
PBS	51	0.873	0.000	0.605	0.547	0.671	−2.441
F_u	46	0.873	0.000	**0.738−**	0.662	0.822	0.008
E	45	0.702	0.000	0.536	0.454	0.633	3.098
Pigeon							
L	30	0.972	0.000	**0.370+**	0.347	0.395	0.680
D_{ml}	30	0.927	0.000	**0.281−**	0.253	0.312	−0.126
D_{dv}	30	0.913	0.000	**0.244−**	0.217	0.273	0.003
CSA	30	0.514	0.000	**0.276−**	0.212	0.361	−0.015
I_{max}	30	0.832	0.000	**0.763−**	0.652	0.894	−0.958
I_{min}	30	0.895	0.000	**0.830−**	0.732	0.941	−1.273
I_{ml}	30	0.886	0.000	**0.841−**	0.738	0.958	−1.266
I_{dv}	30	0.835	0.000	**0.750−**	0.642	0.877	−0.952
J	30	0.863	0.000	**0.788−**	0.683	0.910	−0.787
BS_{ml}	30	0.568	0.000	**0.289−**	0.225	0.372	−1.518
BS_{dv}	30	0.436	0.000	**0.274−**	0.206	0.365	−1.719
PBS	30	0.568	0.000	**0.291−**	0.226	0.374	−1.804
F_u	30	0.846	0.000	**1.229+**	1.056	1.430	−1.526
E	30	0.859	0.000	2.395	2.072	2.768	−2.498

Bold values marked with "+" or "−" indicate significant positive allometry or negative allometry, respectively.
n, sample size; R^2, correlation of the variables; *b*, slope of allometry; LowCI, lower boundary of 95% confidence intervals; UppCI, upper boundary of 95% confidence intervals; Interc, intercept; *L*, bone length; D_{ml}, medio-lateral periosteal diameter of diaphysis; D_{dv}, dorso-ventral periosteal diameter of diaphysis; CSA, cross-sectional area; I_{max}, second moment of area around minor axis; I_{min}, second moment of area around major axis; I_{ml}, second moment of area around medio-lateral axis; I_{dv}, second moment of area around dorso-ventral axis; *J*, polar moment of area; BS_{ml}, bone structural strength index around medio-lateral axis; BS_{dv}, bone structural strength index around dorso-ventral axis; PBS, polar bone structural strength index; F_u, ultimate load; *E*, Young's modulus.

absolute locomotor capabilities. They always need to move at a relatively higher speed than adults do to maintain the same absolute speed, which creates relatively greater loads on their limbs (Carrier, 1996; Herrel & Gibb, 2006; Main & Biewener, 2006; Stevens et al. 2018). In addition, the immature sensory motor system might also create unpredictable locomotor loads (Carrier, 1996). Variable hind limb loads cause juveniles to locomote with low load predictability, weakening the absolute strength of their bones. In summary, juvenile quails suffer relatively larger and more variable hind limb loads compared with adults. Their relatively high femoral mechanical performance corresponds well to the high locomotor functional demands during early ontogeny. With growth, the requirements for robust bones decrease as the disadvantages of immature characteristics diminish. It is uneconomical to maintain a high femoral mechanical performance in adulthood (Dumont, 2010; Blob et al. 2014). Consequently, the negative allometry of femoral mechanical performance correlated with changing functional demands.

In contrast, although juvenile pigeons suffer from the inherent disadvantages of youth, their functional demands for locomotor capability are far lower than juvenile quails because juvenile pigeons enjoy a high degree of parental care. Young pigeons use their hind limbs to compete with siblings and for other in-nest activities, but there is no need to enhance long-bone performance for such low-intensity activities. Consequently, the different ontogenetic patterns of femoral mechanical performance between quails and pigeons result mainly from different functional demands.

© 2019 Anatomical Society

Femoral mechanical performance depends on both material and structural properties. In quails, Young's modulus of 6-day-old birds is already 42% that of adults, and it increased by only 1.4 times throughout ontogeny. However, although PBS, CSA, *I* and *J* scale isometrically against body mass (Table 1), they are far below the scaling relationships required to keep stress constant ($CSA \propto M^{1.0}$, $I \propto M^{1.67}$, $J \propto M^{1.67}$, $BS \propto M^{1.0}$; Biewener, 1982; Main & Biewener, 2006). Consequently, femoral mechanical performance in quails decreases relatively with age, but predictability increases as well. In contrast, in pigeons, PBS, CSA, *I* and *J* show strong negative allometry, whereas Young's modulus increases dramatically with age (140 times). Therefore, although structural resistance decreases relatively with growth, the femoral mechanical performance scales positively against body mass.

Precocial quails and altricial pigeons exhibit extremely different ontogenetic characteristics in femoral Young's modulus, mainly because of different developmental levels in neonatal bones. Although Young's modulus of long bones is similar across adult vertebrates (Biewener, 1982; Currey, 2002; Erickson et al. 2002), neonatal long bones are characterized by different material properties among different taxa (Ricklefs, 1979). The developmental level of neonatal long bones, therefore, has a significant effect on the ontogenetic trajectory of bone material properties.

The negative allometry of bone cross-sectional geometry, which is treated as structural compensation (Carrier, 1983; Carrier & Leon, 1990), is observed in altricial pigeons but not in precocial quails (Table 1), whose femoral performance requirement is obviously greater than in pigeons. However, juvenile quail femora have resistant material properties (6 days: 7.7 GPa, and according to Sliva et al. (2005), Young's modulus of wet femora is about two-thirds that of dry femora, which is 5.1 GPa). Pigeons do not have such stiff femora until ~ 4 weeks (6.1 GPa). The absence of structural compensation in juvenile quails may thus be because of their well-developed bone tissue. Additionally, the negative allometry of femoral ultimate load of quails also suggested that the immature femoral tissue is stiff enough to perform activities normally, even without structural compensation. In contrast, bone material properties of juvenile pigeons are too weak for high femoral mechanical performance, but the presence of structural compensation diminishes the disadvantages caused by weak tissue.

Ontogenetic changes in cross-sectional circularity

The femoral principal circularity of quails is similar in all the ontogenetic stages, whereas pigeons less than 2 weeks old have a larger femoral principal circularity compared with older pigeons. The neonatal limb bone geometry depends on genetic effects, rather than environmental factors, because the neonatal birds rarely locomote. In addition, it is determined by both genetics and hind limb loads in birds that can locomote (Carlson & Judex, 2007; Canington et al. 2018). Juvenile pigeons cannot stand until about 1 week of age. The change in circularity occurs shortly after the birds can locomote; it thus seems likely to be related to locomotor loads.

The anatomical circularity of pigeon femora suggests a higher SMA in medio-lateral orientation than in dorso-ventral direction. However, because of the crouched posture of the hind limbs and the subhorizontal position of femora (Gatesy & Biewener, 1991; Blob, 2000), the femoral load is mainly oriented in dorso-ventral direction. Although $I_{ml} < I_{dv}$, the growth rate ($b = 0.841$) of the I_{ml}, whose orientation is identical to the load direction, is higher than that of I_{dv} ($b = 0.750$). Therefore, the change in circularity may be because of the adaptation of bone cross-sectional geometry to loading.

Studies have observed divergent orientation between the maximum SMA and hind limb loads in both birds and mammals (Cubo & Casinos,1998; Lieberman et al. 2004). These results suggest that the relationship between bone cross-sectional geometry and hind limb loads is indirect (except for some species with specific load contexts, e.g. swimming turtles; Young & Blob, 2015). It is unreasonable to attribute bone geometry to one factor when bone geometry is influenced by several factors (Blob, 2000; Currey, 2003). However, geometric changes might provide some information about hind limb loads. Previous studies observed that the long-bone SMA along the load direction increased rapidly relative to SMA along other directions during ontogeny (Carlson & Judex, 2007; Nadell, 2017; Canington et al. 2018). Therefore, the change in circularity might be an effective indicator of hind limb loads.

Quails have constant circularity during ontogeny. They can locomote within a few hours after hatching. However, the youngest quails we used in this study were 2 days old, and their femoral shapes were probably already affected by the hind limb loads. We could not confirm whether newly hatched quails have different femoral circularity, but the femoral circularity does remain constant in quails from at least 2 days after hatching to adulthood. Terrestrial walk is the primary locomotor pattern throughout a quail's lifetime, and the constant bone circularity may be because of this constant locomotor pattern. Anatomical circularity indicated a larger SMA in dorso-ventral direction than in medio-lateral directions. Quails generally move their hind limbs in a parasagittal plane, which, coupled with the subhorizontal femoral posture, may cause a high magnitude load in the dorso-ventral direction (Gatesy & Biewener, 1991; Blob, 2000). The high I_{ml} of quail femora, thus, has a positive effect on femoral load resistance. However, without phylogenetic data, we cannot confirm whether the high I_{ml} is a true adaptation to terrestrial locomotion.

© 2019 Anatomical Society

Ontogenetic patterns of bone cross-sectional geometry across species

Studies have considered negative allometry of bone cross-sectional geometry as a general ontogenetic trend across most mammal taxa (Carrier, 1996; Herrel & Gibb, 2006), where in birds mainly two allometric patterns have been observed. In California gulls (Carrier & Leon, 1990), black noddies (Bennett, 2008) and pigeons (this study), the cross-sectional geometry of hind limb bones scaled negatively against body mass, whereas in emus (Main & Biewener, 2006, 2007), greater rhea (Picasso, 2011) and Japanese quails (this study), isometry or slight positive allometry was observed (Fig. 3). As mentioned earlier, the different bone material properties of newly hatched birds might have significant effects on their cross-sectional geometry. However, although California gulls (no accurate allometric data of black noddies available) show a negative allometry in bone cross-sectional geometry, the scaling slope of the skeletal Young's modulus (femur, b = 1.264; tibiotarsus, b = 0.803; tarsometatarsus, b = 0.853; Carrier & Leon, 1990) is obviously lower compared with pigeons (b = 2.395). In addition, we cannot simply use the developmental extent of neonatal bone tissue to explain why most mammals share a similar scaling relationship in bone cross-sectional geometry because structural compensation is found in both precocial and altricial mammals (e.g. hares, muskoxen, brown rats and goats; Carrier, 1983; Heinrich et al. 1999; Lammers & German, 2002; Main & Biewener, 2004).

Main & Biewener (2004, 2006, 2007) suggested that different bone growth patterns between goats and emus essentially result from different selection pressures caused by different threat avoidance strategies of young individuals. Therefore, essentially, different ontogenetic patterns of bones result from different functional demands. In birds, it is not difficult to consider that species with similar allometric patterns might also share similar locomotor behaviours. California gulls, black noddies and pigeons, which showed negative allometry in bone cross-sectional geometry, develop from hind limb-dominated juveniles into forelimb-dominated adults. The negative allometry in hind limb bone geometry corresponds to the decreasing importance of hind limbs in locomotion during ontogeny. In contrast, emus and greater rhea are both flightless. Although quails can fly once fully grown, they prefer to run from threats rather than fly (Ricklefs, 1979). Legs are thus the primary locomotor organs throughout their lifetime. The isometric increase in bone geometry corresponds well to the constant high locomotor functional demands on the hind limbs during ontogeny.

Birds' unique characteristics and specialisations for flying and bipedalism may contribute to their different bone ontogenetic patterns. Birds have three locomotor modules: wings, hind limbs and tails. These modules offer birds more locomotor options and, therefore, various limb designs and locomotor strategies (Gatesy & Dial, 1996). Furthermore, flight may ease the constraints on the hind limbs; diverse locomotion may also result in various long-bone ontogenetic patterns (Gatesy & Middleton, 1997). Compared with birds, mammals locomote in more uniform ways, and most mammals use running as the primary locomotor behaviour. Although limbs exhibit various behaviours such as digging and hopping in some species, limb structure will undoubtedly reserve its primary function in support and terrestrial locomotion which may pose constraints on limb design and lead to less specialization that is not as strong as flying in birds (Gatesy & Dial, 1996; Jackson et al. 2009). In addition, the mammals examined in bone ontogenetic studies so far are almost all terrestrial species (e.g. lagomorphs, muskoxen, rodents and goats; Carrier, 1983; Heinrich et al. 1999;

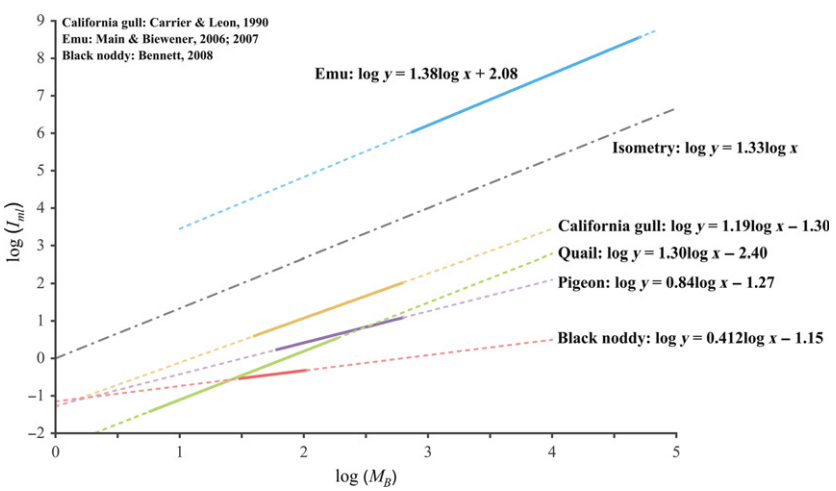

Fig. 3 Ontogenetic scaling of the second moment of area around medio-lateral axis (I_{ml}) vs. body mass (M_B) in some ground-dwelling and flying birds. The solid lines represent the actual log body mass range of the birds, and dotted lines are extension lines made for comparison.

© 2019 Anatomical Society

Lammers & German, 2002; Main & Biewener, 2006). Their similar locomotor behaviour might cause them to share uniform cross-sectional ontogenetic patterns of limb bones.

According to biomechanical principles, an equilibrium in relationship is expected among bone material properties, bone structural properties and functional demands, where the synergy of bone material and structural properties meets functional demands. Among them, bone structural properties might be most flexible, as these are easily modified to keep the relationship in equilibrium. Moreover, bone structural properties are always the primary variable in determining bone strength, whereas bone material properties are considered similar across adult vertebrates (Selker & Carrier, 1989; Erickson et al. 2002; Currey, 2003). However, as mentioned earlier, bone cross-sectional geometry has no straightforward relationship with hind limb load. Fortunately, geometric changes, especially ontogenetic geometric changes, might effectively inform us about animal behaviours.

Conclusions

This study showed that femora of quails and pigeons undergo very different growth patterns in their structural and mechanical traits during postnatal ontogeny. The mechanical performance of femora exhibited negative allometry in quails but positive allometry in pigeons, which is clearly related to the precocial and altricial species' decreasing and increasing functional demands for hind limbs during growth, respectively. Judged by the negative allometric growth of the femoral cross-sectional geometry, the femur of young pigeon is relatively robust, to compensate for the weak material properties of skeletal tissue, and to ensure its mechanical performance before adulthood. During ontogeny, the complementary relationship between structural and material characteristics might be common in altricial and semi-altricial birds, but to reach a solid conclusion, more comparative works across a broad range of avian species are necessary. As reported in other flying and ground-dwelling birds, growth of the femoral cross-sectional geometry in pigeon and quail presented a negative allometric and isometric pattern, respectively; this kind of correspondence between shape change and principal mode of locomotion is useful to better understand the movement and behaviour of fossil birds. Unlike quails, significant changes of femoral circularity accompanying the onset of locomotion were found in pigeons. This finding suggests that the dynamic of circularity, not the circularity itself, may reflect the loading condition of the hind limb.

Acknowledgements

We are grateful to Qunbo Fan and Tao Sun for technical support; to our lab members for helping on data collection; enago for language editing services; two anonymous reviewers for their useful and detailed suggestions, which greatly improved this manuscript. This work was supported by the National Natural Science Foundation of China (No. 31471951).

Conflict of interest

The authors declare no conflict of interests.

Authors' contributions

X.W. and Z.Z. conceived and designed the study. X.W. collected and analysed data and prepared the figures. X.W. and Z.Z. wrote the manuscript.

References

Abourachid A, Höfling E (2012) The legs: a key to bird evolutionary success. *J Ornithol* **153**, 193–198.

Bennett MB (2008) Post-hatching growth and development of the pectoral and pelvic limbs in the black noddy, *Anous minutus*. *Comp Biochem Physiol A Mol Integr Physiol* **150**, 159–168.

Biewener AA (1982) Bone strength in small mammals and bipedal birds: do safety factors change with body size? *J Exp Biol* **98**, 289–301.

Blob RW (2000) Interspecific scaling of the hindlimb skeleton in lizards, crocodilians, felids and canids: does limb bone shape correlate with limb posture? *J Zool* **250**, 507–531.

Blob RW, Biewener AA (1999) *In vivo* locomotor strain in the hindlimb bones of *Alligator mississippiensis* and *Iguana iguana*: implications for the evolution of limb bone safety factor and non-sprawling limb posture. *J Exp Biol* **202**, 1023–1046.

Blob RW, Espinoza NR, Butcher MT, et al. (2014) Diversity of limb-bone safety factors for locomotion in terrestrial vertebrates: evolution and mixed chains. *Integr Comp Biol* **54**, 1058–1071.

Canington SL, Sylvester AD, Burgess ML, et al. (2018) Long bone diaphyseal shape follows different ontogenetic trajectories in captive and wild gorillas. *Am J Phys Anthropol* **167**, 366–376.

Carlson KJ, Judex S (2007) Increased non-linear locomotion alters diaphyseal bone shape. *J Exp Biol* **210**, 3117–3125.

Carrier DR (1983) Postnatal ontogeny of the musculo-skeletal system in the Black-tailed jack rabbit (*Lepus californicus*). *J Zool* **201**, 27–55.

Carrier DR (1996) Ontogenetic limits on locomotor performance. *Physiol Zool* **69**, 467–488.

Carrier DR, Leon LR (1990) Skeletal growth and function in the California gull (*Larus californicus*). *J Zool* **222**, 375–389.

Cubo J, Casinos A (1998) Biomechanical significance of cross-sectional geometry of avian long bones. *Eur J Morphol* **36**, 19–28.

Currey JD (2002) *Bones: Structure and Mechanics*. Princeton: Princeton University Press.

Currey JD (2003) The many adaptations of bone. *J Biomech* **36**, 1487–1495.

Doube M, Klosowski MM, Arganda-Carreras I, et al. (2010) BoneJ: Free and extensible bone image analysis in ImageJ. *Bone* **47**, 1076–1079.

Dumont ER (2010) Bone density and the lightweight skeletons of birds. *Proc R Soc B* **277**, 2193–2198.

© 2019 Anatomical Society

Dytham C (2003) *Choosing and Using Statistics: A Biologist's Guide*. Oxford: Blackwell Publishing.

Erickson GM, Catanese J 3rd, Keaveny TM (2002) Evolution of the biomechanical material properties of the femur. *Anat Rec* **268**, 115–124.

Gatesy SM, Biewener AA (1991) Bipedal locomotion: effects of speed, size and limb posture in birds and humans. *J Zool* **224**, 127–147.

Gatesy SM, Dial KP (1996) Locomotor modules and the evolution of avian flight. *Evolution* **50**, 331–340.

Gatesy SM, Middleton KM (1997) Bipedalism, flight, and the evolution of theropod locomotor diversity. *J Vert Paleontol* **17**, 308–329.

Habib MB, Ruff C (2008) The effects of locomotion on the structural characteristics of avian limb bones. *Zool J Linn Soc* **153**, 601–624.

Heinrich RE, Ruff CB, Adamczewski JZ (1999) Ontogenetic changes in mineralization and bone geometry in the femur of muskoxen (*Ovibos moschatus*). *J Zool* **247**, 215–223.

Herrel A, Gibb AC (2006) Ontogeny of performance in vertebrates. *Physiol Biochem Zool* **79**, 1–6.

Jackson BE, Segre P, Dial KP (2009) Precocial development of locomotor performance in a ground-dwelling bird (*Alectoris chukar*): negotiating a three-dimensional terrestrial environment. *Proc R Soc B* **276**, 3457–3466.

Jepsen KJ, Silva MJ, Vashishth D, et al. (2015) Establishing biomechanical mechanisms in mouse models: practical guidelines for systematically evaluating phenotypic changes in the diaphyses of long bones. *J Bone Miner Res* **30**, 951–966.

Lammers AR, German RZ (2002) Ontogenetic allometry in the locomotor skeleton of specialized half-bounding mammals. *J Zool* **258**, 485–495.

Lanyon LE (1980) The influence of function on the development of bone curvature. An experimental study on the rat tibia. *J Zool* **192**, 457–466.

Lieberman DE, Polk JD, Demes B (2004) Predicting long bone loading from cross-sectional geometry. *Am J Phys Anthropol* **123**, 156–171.

Main RP, Biewener AA (2004) Ontogenetic patterns of limb loading, *in vivo* bone strains and growth in the goat radius. *J Exp Biol* **207**, 2577–2588.

Main RP, Biewener AA (2006) *In vivo* bone strain and ontogenetic growth patterns in relation to life-history strategies and performance in two vertebrate taxa: goats and emu. *Physiol Biochem Zool* **79**, 57–72.

Main RP, Biewener AA (2007) Skeletal strain patterns and growth in the emu hindlimb during ontogeny. *J Exp Biol* **210**, 2676–2690.

Nadell JA (2017) Ontogeny and Adaptation: A Cross-Sectional Study of Primate Limb Elements. PhD Thesis, Durham University.

Picasso MBJ (2011) Postnatal ontogeny of the locomotor skeleton of a cursorial bird: greater rhea. *J Zool* **286**, 303–311.

Ricklefs RE (1979) Patterns of growth in birds. V. A comparative study of development in the starling, common tern, and Japanese quail. *Auk* **96**, 10–30.

Ruff CB (2003) Growth in bone strength, body size, and muscle size in a juvenile longitudinal sample. *Bone* **33**, 317–329.

Ruff CB, Holt B, Trinkaus E (2006) Who's afraid of the big bad Wolff?: 'Wolff's law' and bone functional adaptation. *Am J Phys Anthropol* **129**, 484–498.

Selker F, Carrier DR (1989) Scaling of long bone fracture strength with animal mass. *J Biomech* **22**, 1175–1183.

Silva MJ, Brodt MD, Hucker WJ (2005) Finite element analysis of the mouse tibia: estimating endocortical strain during three-point bending in SAMP6 osteoporotic mice. *Anat Rec* **283**, 380–390.

Spatz H-CH, O'Leary EJ, Vincent JFV (1996) Young's moduli and shear moduli in cortical bone. *Proc R Soc B* **263**, 287–294.

Stevens LM, Blob RW, Mayerl CJ (2018) Ontogeny, morphology and performance: changes in swimming stability and turning performance in the freshwater pleurodire turtle, *Emydura subglobosa*. *Biol J Linn Soc* **125**, 718–729.

Young VKH, Blob RW (2015) Limb bone loading in swimming turtles: changes in loading facilitate transitions from tubular to flipper-shaped limbs during aquatic invasions. *Biol Lett* **11**, 20150110.

© 2019 Anatomical Society